

Preliminary Analysis of the Failure Process of a Tailings Dam

Jiarui Chen, University of California, Davis, USA

Alfonso Cerna-Diaz, AECOM, USA

Scott M. Olson, University of Illinois at Urbana-Champaign, USA

Abstract

Motivated by recent high-profile tailings storage facility (TSF) failures around the globe, the tailings and mine waste community is actively working to identify potential triggering mechanisms for those tragedies. Case histories are a valuable resource to understand triggering mechanisms. This paper presents a preliminary analysis of a tailings dam failure that occurred over two decades ago, which released about 283,000 cubic meters of tailings and non-mineralized mine rock along a 274-meter-long section of the west-facing slope. The released mass flowed downstream for about 610 meters. The failure took place at a location where waste rock was being placed on top of tailings. Specifically, the rapid placement of a second 15-meter lift of waste rock likely led to an undrained failure in the tailings due to a lack of time for excess porewater pressure (PWP) dissipation.

In this study, limit equilibrium (LE) analysis was adopted. Excess PWP within the tailings before the triggering of the failure was taken into account by assigned B -bar values. In addition, a LE analysis strategy considering strength reduction and failure surface evolution (from a local rotational shear failure to a global breach) was performed to understand the progression of the failure. Analysis results highlighted the following two key aspects: (1) the failure was correctly captured through LE analysis when the drainage conditions, or the excess PWP, was well quantified; and (2) a reasonable progression of the failure can be verified through LE analysis considering strength loss in the tailings. These findings affirm the capability of the LE analysis despite its simplicity. Furthermore, this study provides a valuable case to expand the current case history-based liquefaction flow failure database.

Introduction

Limit equilibrium (LE) analysis has been widely utilized in the initial design for sloping ground structures and also for back-calculation of liquefaction flow failure case histories (Olson and Stark, 2002). The general procedure for using the LE analysis involves inputting strength parameters for soils. The undrained strength

ratio method, where undrained shear strength is normalized by the initial effective vertical stress, is popular because it simplifies strength assignment in compressible materials that are susceptible to liquefaction (such as many tailings), where the critical state line is reasonably parallel to the normal consolidation line. However, one issue with using an undrained strength ratio to evaluate staged construction (or any ongoing construction such as is common in tailings storage facility [TSF] construction) in LE analysis is related to how loads are input and stresses are computed. As widely understood in soil mechanics, an increase in vertical stress generates excess porewater pressure (PWP) in underlying soil layers. In LE analysis, placing an additional soil layer or surface pressure increases the total and effective vertical stress (consolidation is assumed to be complete), which in turn increases the undrained shear strength computed using a strength ratio and artificially increases the factor of safety. This issue with staged construction can be addressed using the B-bar parameter (Skempton, 1954), as discussed later in the paper, but this approach requires an accurate assessment of construction-induced excess PWP.

In addition, it is not common to utilize the LE analysis to study failure progression because LE analysis usually reports the most critical slip surface, and that may only represent part of the entire failure process in the field. Furthermore, LE analysis does not support advanced constitutive modelling to consider the development and potential loss of shearing resistance as well as shear strain accumulation and propagation. However, due to its efficiency and simplicity, the method remains the workhorse for stability analysis.

In this study, we performed LE analyses to evaluate a copper TSF failure, focusing on two aspects: (1) incorporation of the excess PWP in the saturated tailings due to construction loading; and (2) how to effectively use LE analysis to understand failure progression.

Description of the failure

The TSF failure investigated in the current study happened over 20 years ago and is documented in Chen (2022). The failure itself reportedly occurred over a 30-minute period, releasing approximately 283,000 cubic meters (370,000 cubic yards) of tailings and non-mineralized waste rock along an approximately 274-meter-long (900-ft) section. The failure initiated within the original tailings impoundment, which served as the foundation for a waste rock dump that was being constructed. Initially, a 15-meter-thick (50-ft) lift of waste rock was placed at the location of the failure. The lift took about 30 days to place and was followed by a 20-day resting period. When the second 15-meter-thick (50-ft) lift was being placed, the failure was triggered. The flowing mass, which consisted of the waste rock and saturated tailings, flowed down the valley slope approximately 610 meters (2,000 ft). Figure 1 illustrates the failure. Fortunately, no injuries occurred during this failure.

Along the valley slope, many sand boils were observed in the failed tailings. The sand boils dried up one week after the failure. Piezocone penetration test (CPTu) soundings were advanced at locations about

30.5 to 61 meters (100 to 200 feet) back from the main scarp of the failure. The measured piezometric surface elevations from those CPTu soundings indicated excess PWP of about 15.2 to 19.8 meters (50 to 65 ft) within the tailings. It could be easily inferred that high excess PWP existed in the saturated tailings at the time of the failure, and the resulting static liquefaction was triggered due to this high excess PWP.

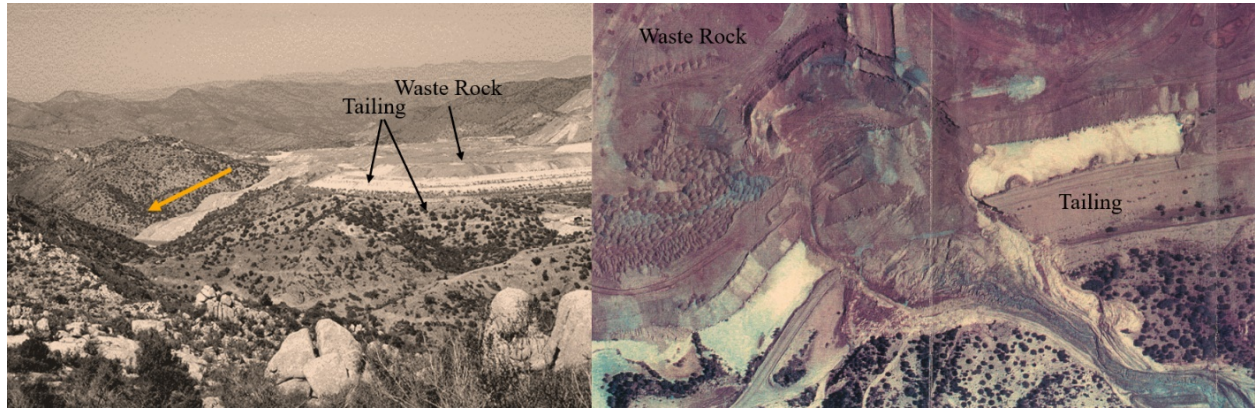


Figure 1: Photos of TSF failure. Left: oblique photo showing runoff and waste rock; Right: Aerial photo showing scarp and runoff

Soil characterization

At this site, tailings were deposited by spigotting from perimeter tailings discharge pipes. The dams were raised upstream using the deposited tailings to construct the perimeter embankment. The tailings involved in the failure was found to be loose to very loose, non-plastic silty sands to silts (SM or ML), with fines contents ranging from 40 – 90% and a specific gravity of 2.65.

Both pre- and post-failure CPTu soundings were performed within the impoundment and near the crest within the coarse tailings area, i.e., the perimeter embankment. Figure 2 presents representative CPTu results. Figure 2 (a) illustrates the pre-failure CPTu profile closest to the failure location. The tip resistance of the fine tailings is generally in the range of about 1.1 to 2.1 MPa (10 to 20 tsf), indicating a relatively low strength. Moreover, according to Robertson (2010, 2016), the majority of the fine tailings within the impoundment can be classified as Sensitive Contractive Fines. In addition, Figure 2 (a) and (c) both illustrate the fact that the fine tailings behaves contractively, generally with a positive state parameter (Been and Jefferies, 1985) and positive penetration-induced excess PWP. CPTu soundings also were conducted in the coarse tailings near the crest, as illustrated in Figure 2 (b). Although the tip resistance can be much higher within the coarse tailings to a depth of about 24 m (80 ft), reaching values up to 10.7 MPa (100 tsf), interbedded weak layers were encountered. In particular, weak layers are observed at depths of 13.7 m (45 ft), 18 m (59 ft), 19.5 to 21.6 m (64 to 71 ft), consistent with depths where the tip resistances in the impoundment are low (Figure 2 a). This observation suggests a potential continuity of weak layers within

the impoundment, extending as far as the coarse tailings area near the crest. The occurrence of observed global failure may be related to these continuous weak layers that can be identified in the CPTu soundings.

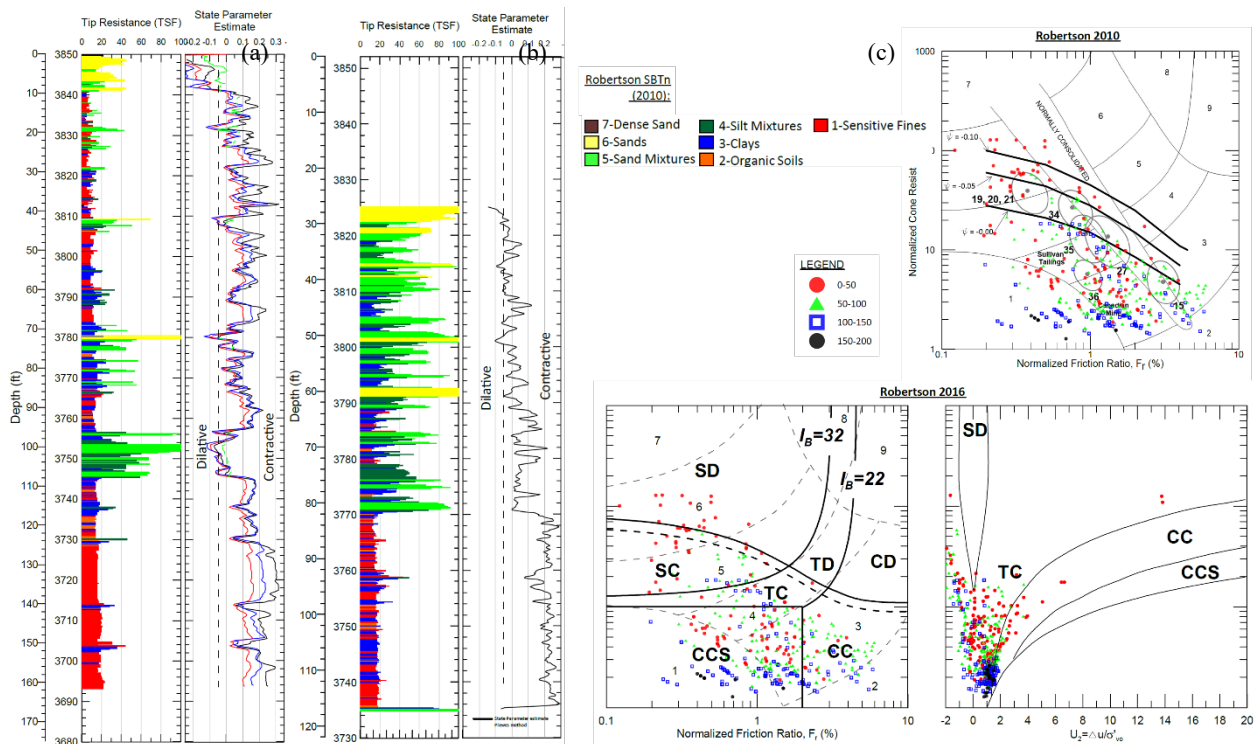


Figure 2: (a) Representative pre-failure CPTu tip resistance and estimated state parameter closest to the failure location; (b) representative post-failure CPTu tip resistance and estimated state parameter within the coarse tailings near the crest close to the failure location; and (c) representative soil behaviour interpretation for the CPTu results shown in (a)

Previous findings in finite element analyses

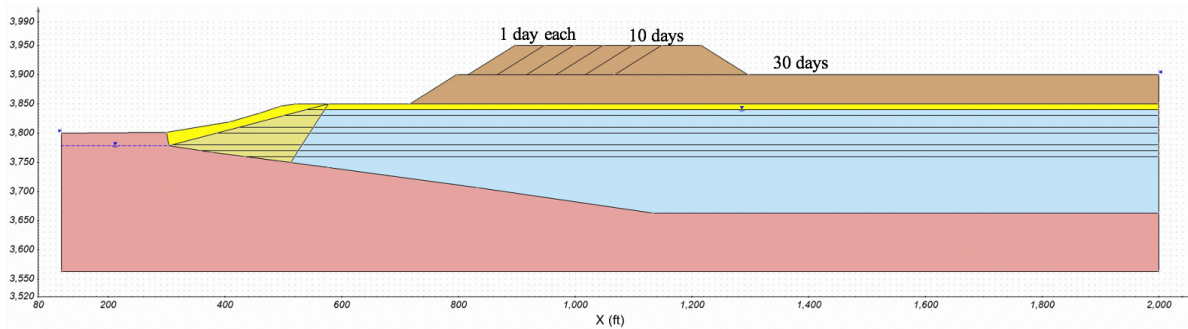


Figure 3: Geometry of the TSF for both the FE and LE analyses, where the annotations indicate the construction time for the waste rock

Cerna-Diaz et al. (2024) conducted fully coupled 2D finite element (FE) modelling of this tailings dam failure using PLAXIS. Figure 3 presents the model geometry. The model accounted for the actual construction sequence in the field prior to failure and allowed for daily dissipation of excess PWP. As

indicated in Figure 3, the first 15-meter-high waste rock lift took about 30 days to construct. Then, a 20-day-resting period was allowed. Following the resting period, a portion of the second lift of waste rock was placed in 10 days (as shown on the right side of Figure 3). Then, five small segments of waste rock were placed in 1 day each. In the FE analysis, the fine tailings was modelled using NorSand (Jefferies, 1993). Table 1 presents the model parameters. For the base case, a single representative state parameter of +0.1 (~80th percentile value) was assigned to the fine tailings based on the CPT widget (Shuttle and Jefferies, 2016) based on the Figure 2 (a) results. Cerna-Diaz et al. (2024) details the FE simulations.

Table 1: NorSand model parameters for the finite element analysis

Material	Γ	λe	Mtc	N	χ	Plastic hardening (H)	Elasticity	Permeability
Fine tailings	0.83	0.061	1.4	0.3	4.6	$H_o=160, H_\psi=56$	$G_{ref}=2.7 \times 10^4 \text{ kPa}$, $n_g=0.37$	$K_x = 0.07 \text{ m/day}$ $K_y = 0.004 \text{ m/day}$

Figure 4 illustrates a representative simulation result. The computed shear strains in the figure indicate that, after the placement of the final five waste rock segments, a rotational shear failure occurred within the impounded tailings foundation and extended through the waste rock lifts. This failure mechanism is consistent with the steep rockfill scarp observed after the failure. Based on the shear strains predicted in the FE model, the authors speculated that the rotational failure deformed a substantial volume of tailings near the TSF crest, which may have triggered liquefaction in the tailings between the rockfill and the perimeter embankment resulting in the TSF breach and the global liquefaction flow slide.

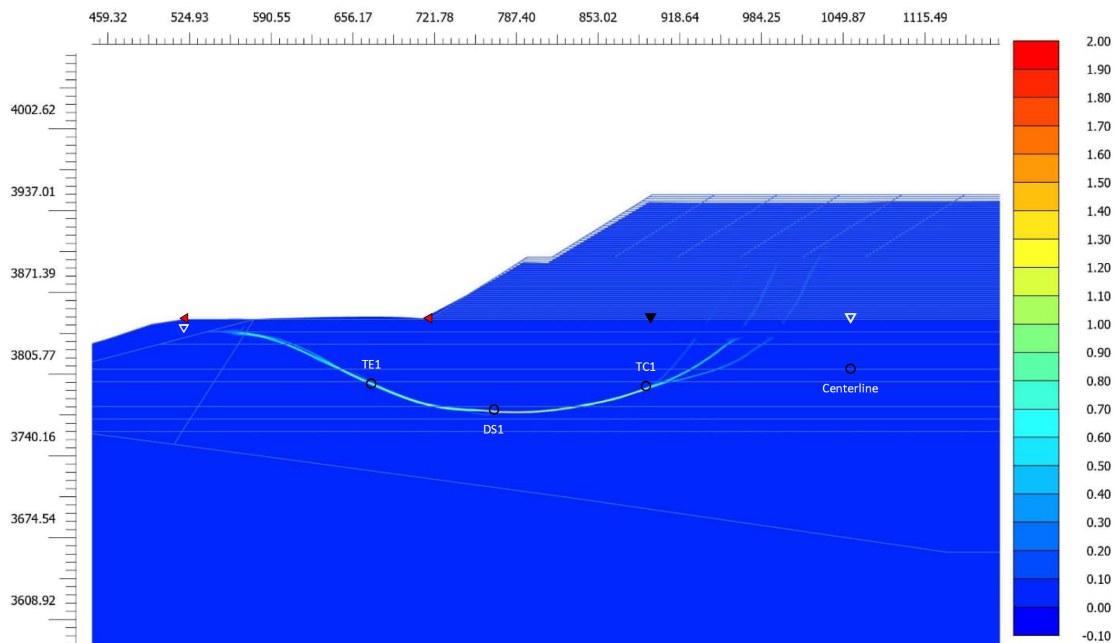





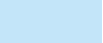

Figure 4: Representative FE analysis results. Legend indicates shear strain magnitudes

Limit equilibrium analyses

Model geometry and material parameters

In addition to advanced numerical techniques for TSF stability study, LE analysis is still widely used due to its efficiency and convenience. Herein, the authors employed LE analyses (using the PLAXIS LE platform) to analyse the same flow failure case history studied by Cerna-Diaz et al. (2024) to verify the capability of the LE analysis. The geometry of the LE model is the same as that used in the FE analysis (see Figure 3). Table 2 provides a detailed description of the material parameters used in the LE analysis. For the coarse and fine tailings, both yield and liquefied shear strength ratios were used to study the failure progression. Note that the liquefied shear strength is referred to elsewhere as the undrained residual shear strength and the post-liquefaction shear strength. To be consistent with the FE analysis, yield and liquefied strength ratios were derived from the Jefferies and Been (2015) NorSand model parameters reported in Table 1. A state parameter of +0.09 was adopted for the coarse tailings, while a value of +0.1 was used for the fine tailings. Other material parameters were assigned to the model using published and unpublished reports (including laboratory data) available to the authors.

Table 2: Limit equilibrium analysis soil properties

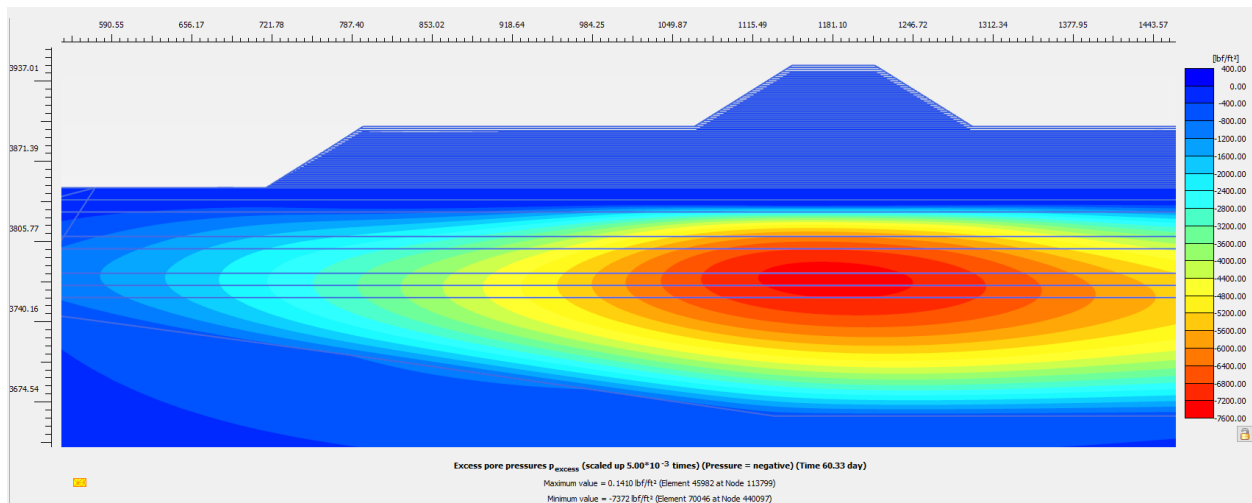
Soil	Colour	Unit weight kN/m ³	Model	Parameters		
				c' kPa	φ' degrees	s _u /σ' _{vo}
Waste rock		20.4	Mohr-Coulomb	0	38	
Coarse tailings		16.5	Mohr-Coulomb	0	34	
Coarse tailings		18.8	Undrained strength ratio			0.26 (Yield) 0.10 (Liquefied)
Fine tailings		18.8	Undrained strength ratio			0.26 (Yield) 0.09 (Liquefied)
			Mohr-Coulomb		34	
Gila foundation		20.4	Mohr-Coulomb	240	45	

Modeling procedure, completed cases, and discussion

Multiple LE scenarios were considered to realistically study the TSF failure. Table 3 compiles the completed scenarios. In Table 3, Day 50 corresponds to the time after the first 15-meter-high waste rock was dumped in place (30 days) and the resting period (20 days). Day 60 corresponds to the completion of the “right hand” segment of the second 15-meter-high lift of waste rock (see Figure 3). Day 65 is the time when the final five segments of the waste rock were completed and the failure was triggered.

Consolidated-undrained conditions at Day 50, 60, and 65 (Case 1 to 3) first were analysed to identify the risk of the waste rock placement and serve as bounding cases for comparison to undrained cases. The resulting factor of safety (FOS) indicates that if sufficient time is allowed for consolidation, the TSF can remain stable under the observed loading. The time required for consolidation depends on material properties (e.g., permeability and coefficient of consolidation), layering, and drainage boundaries, and is best evaluated by instrumentation and monitoring (e.g., piezometers and settlement plates).

Next, the authors considered numerous undrained cases where construction-induced excess PWP generated within the fine tailings at Day 60 were considered. The excess PWP were imported from the FE analysis and are shown in Figure 5. Although allowed some time for consolidation, the excess PWP within the soil was still high due to the low permeability of the fine tailings. As shown in the figure, the excess PWP reached about 364 kPa (7600 psf) below the second lift of the waste rock. If the loading from both lifts is considered, the maximum PWP corresponds to a B-bar value of 0.57. B-bar in the current study was defined as the ratio between the generated excess porewater pressure and the applied total vertical stress, and is based on Skempton (1954). In Cases 4 – 6, no PWP dissipation during the placement of the last five segments was assumed, which corresponds to a fully undrained condition for the final loading stages. New excess PWP were calculated using the excess PWP at Day 60 and the loading from the last five waste rock segments. The corresponding B-bar values were calculated using the applied load from both waste rock lifts to take into account the existing excess PWP at Day 60. In PLAXIS LE, the excess PWP generation function was enabled for the fine tailings. The fine tailings were divided into multiple sections to accommodate the horizontal variation in B-bar. Average B-bar were assigned to each section. As a result, the LE model successfully incorporates more realistic partially drained conditions for the LE analysis cases.



**Figure 5: Construction-induced excess PWP at Day 60 from the FE analysis.
(Negative value represents positive excess PWP)**

Table 3: Completed cases for the limit equilibrium analysis

Case No.	Day	Fine tailings undrained strength ratio	Description	Slip surface condition	FOS
1	50	Yield	B-bar = 0	Local	1.20
2	60	Yield	B-bar = 0	Local	1.20
3	65	Yield	B-bar = 0	Local	1.11
4	65	Yield	Consider excess porewater pressure at Day 60 and assume fully undrained loading afterward	Local	0.79
5	65	Yield and liquefied		Global	0.63
6	65	Liquefied only		Global	0.44
7	65	Yield	B-bar = 1	Local	0.60
8	65	Yield and liquefied		Global	0.50
9	65	Liquefied only		Global	0.35
10	65	Yield	B-bar = 0.75	Local	0.78
11	65	Yield and liquefied		Global	0.63
12	65	Liquefied only		Global	0.45
13	65	Yield	B-bar = 0.5	Local	0.93
14	65	Yield and liquefied		Global	0.72
15	65	Liquefied only		Global	0.55
16	65	Yield	B-bar = 0.25	Local	1.01
17	65	Yield and liquefied		Global	0.81
18	65	Liquefied only		Global	0.65
19	65	Not applicable, drained strength assigned	Fully drained	Local	1.20

After constructing the LE model with the desired excess PWP, the LE analysis started with assigning yield strength ratios to the fine tailings to verify whether the local failure could happen. If the local rotational shear failure occurred, a failure progression study then was conducted. Theoretically, with further straining, the strength of the fine tailings will decrease to the liquefied shear strength. This reduction can occur within a shear strain of less than 5% (Jefferies and Been, 2015). Thus, it is reasonable to infer that with further shearing, the fine tailings beneath the waste rock experienced strain softening and ultimately reached the critical state (or the liquefied condition in the field). With the further propagation of the failure, the tailings not involved in the local failure started to experience straining. This could be related to shearing along continuous weak layers (see Figure 2b) underneath the coarse tailings near the crest. A global slip surface that extends from the tailings below the waste rock to the perimeter embankment could be initiated. The fine tailings outside the waste rock area was assigned the yield strength ratio. If the FOS for this case is

less than unity, shear deformation can keep accumulating and the downstream tailings could be triggered to liquefy.

Cases 4 to 6 simulated the described process. It can be found in Table 3 that the FOS for Case 4 is 0.792 (i.e., less than unity). The critical slip surface for Case 4 is shown in Figure 6 (a). The predicted local rotational shear failure below the waste rock is consistent with the observed failure scarp. Furthermore, the critical slip surface identified in Figure 6 (a) matched very well the location of the zone of high shear strain from the FE analysis (Figure 4). This provided confidence in the LE analysis results under partially drained conditions, despite the simplified procedure for assigning B-bar.

After completing Case 4, failure progression analyses were also conducted (Cases 5 and 6). Figure 6 (b) presents the adopted global critical slip surface. The FOS of Cases 5 and 6 are 0.63 and 0.44, respectively. Particularly, the FOS of 0.63 indicates that the tailings near the perimeter crest was not strong enough to sustain the transferred shearing and also should have liquefied. Combining Cases 4 to 6, it seems to be reasonable to conclude that although the failure may have been initiated within the impoundment beneath the waste rock, if the shear deformation extended downstream, particularly if continuous weak layers were present, a global failure consistent with the observed liquefaction flow failure would be predicted.

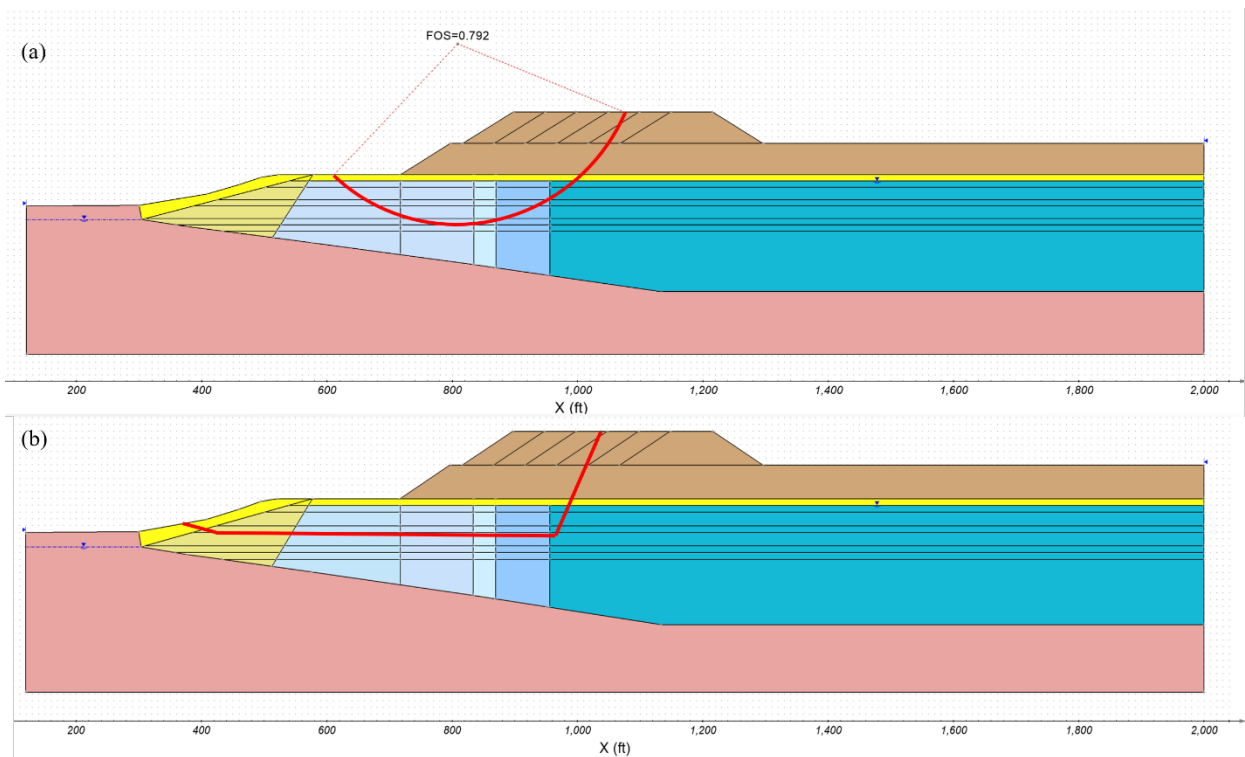


Figure 6: (a) Local critical slip surface for Case 4 with FOS = 0.79; and (b) Global slip surface Case 5 and 6 with FOS = 0.63 and 0.44, respectively. Different colours for fine tailings beneath the waste rock represent different B-bar values assigned

The described procedure for modelling the initiation and progression of the failure also was adopted to systematically evaluate the influence of the B-bar variation within the fine tailings, in other words, the degree of drainage that occurred in the fine tailings. One single B-bar value was assigned to the fine tailings and varied from 0 to 1 (Cases 3 and Cases 7 – 18). The local failure FOS for these Cases ranged from 0.6 to 1.11. With further shearing and failure progression, the FOS considering strength reduction further decreases, as can be seen in Table 3. The scenario that the fine tailings mobilized a drained shear strength was also conducted (Case 19) for comparison purpose only. A much larger FOS was obtained for this fully drained condition, suggesting that with proper design, construction, and monitoring, it is possible to safely place waste rock on tailings impoundments.

The variation in local slip surface FOS for various B-bar emphasizes the importance of properly considering the potential excess PWP generation. When loading is applied rapidly, as in the subject case, the driving stress, which is a function of the total stress, could be large enough to trigger liquefaction and induce slope instability. In addition, ignoring the existing excess PWP potentially can bias the strength back-calculated from a liquefaction flow failure case history.

Conclusion

This study presents LE analyses of a well-documented TSF failure considering multiple PWP and shear strength scenarios. To achieve that, 19 cases were evaluated. Two major conclusions can be made from the current study, as follows.

1. The excess PWP within the saturated tailings is particularly important for identifying whether the failure can occur. With proper incorporation of excess PWP, the LE analysis of the subject case history was able to capture the initiation of the slope failure. And the predicted rotational shear failure initiated beneath the waste rock, consistent with advanced FE analysis results described by Cerna-Diaz et al. (2024).
2. With a reasonable strategy, the LE analysis is capable of verifying the failure progression, from local to global, despite its simplicity. When the occurrence of a global failure is known but the LE analysis only provides a local critical slip surface with FOS less than unity, it may be reasonable to extend the local critical slip surface downstream to incorporate the soil that needs to fail to induce a global breach. Notably, strength reduction from yield shear strength to liquefied shear strength near the original local critical slip surface may need to be considered.

Although this study highlighted the benefits of LE analysis, LE analysis is still subject to several limitations, including accounting for strength anisotropy and providing a detailed explanation for how the

failure propagated and extended the local slip surface to a global slip surface. Further research on these topics is ongoing. In addition, the potential 3D effect of the failure is also of interest.

References

- Been, K., and M. Jefferies. 1985. A state parameter for sands. *Géotechnique* 35(2): 99–112. Available at: <https://doi.org/10.1680/geot.1985.35.2.99>.
- Cerna-Diaz, A., S.M. Olson, J. Chen and T. Barham. 2024. Role of permeability on static liquefaction of tailings dams. 2024 USSD Annual Conference and Exhibition. In review.
- Chen, J. 2022. An investigation of liquefied shear strength using novel centrifuge tests, direct simple shear tests, and field case histories. Doctoral thesis, University of Illinois at Urbana-Champaign. Available at: <https://www.ideals.illinois.edu/items/126546>
- Jefferies, M.G. 1993. Nor-Sand: a simple critical state model for sand. *Géotechnique*, 43(1): 91–103. ICE Publishing. Available at: <https://doi.org/10.1680/geot.1993.43.1.91>.
- Jefferies, M. and K. Been. 2015. *Soil Liquefaction: A Critical State Approach, Second Edition*. London: CRC Press.
- Olson, S.M. and T.D. Stark. 2002. Liquefied strength ratio from liquefaction flow failure case histories. *Canadian Geotechnical Journal* 39 (3): 629–647. Available at: <https://doi.org/10.1139/t02-001>.
- Robertson, P.K. 2010. Evaluation of flow liquefaction and liquefied strength using the cone penetration test. *Journal of Geotechnical and Geoenvironmental Engineering*, 136 (6): 842–853. [https://doi.org/10.1061/\(ASCE\)GT.1943-5606.0000286](https://doi.org/10.1061/(ASCE)GT.1943-5606.0000286).
- Robertson, P.K. 2016. Cone penetration test (CPT)-based soil behaviour type (SBT) classification system — an update. *Canadian Geotechnical Journal* 53(12): 1910–1927. Available at: <https://doi.org/10.1139/cgj-2016-0044>.
- Shuttle, D. and M. Jefferies. 2016. Determining silt state from CPTu. *Geotechnical Research* 3(3): 90–118. Available at: <https://doi.org/10.1680/jgere.16.00008>.
- Skempton, A.W. 1954. The pore-pressure coefficients A and B. *Géotechnique* 4(4): 143–147. ICE Publishing. Available at: <https://doi.org/10.1680/geot.1954.4.4.143>.

